Periodica Polytechnica
Civil Engineering

61(3), pp. 541–547, 2017
https://doi.org/10.3311/PPci.10169

RESEARCH ARTICLE

Investigation of Frost-Heaving Characteristics of Horizontal-Cup-Shape Frozen Ground Surface for Reinforced End Soil Mass in Shield Tunnel Construction

Ting Zhang[1], Ping Yang[1], Yongxing Zhang [1,*]

Received 16 October 2016; Accepted 07 December 2016

Abstract

Artificial freezing method is commonly adopted for reinforcing end soil mass of shield tunnel in the weak and rich aqueous formation, which is expected to prevent the construction risk in the originating and arriving of shield machine, whereas the arrangement of freezing pipes is sometimes varied due to various complex limitations, and the corresponding frost-heaving characteristics of ground surface also differs from others. In this paper, a case of artificial freezing end soil mass with cup shape arrangement of horizontal freezing pipes is studied by field investigation and numerical analysis, in which a numerical model coupled with water-heat-force interactions is proposed for appropriately evaluating the frost-heaving characteristics of ground surface in artificial freezing method. The results demonstrate that all the considered factors on brine temperature, buried depth and cup bottom thickness have significantly influences of frost-heaving characteristics of ground surface in the artificial ground freezing (AGF) with cup shape arrangement of horizontal freezing pipes, in which the frost heave displacement of horizontal-cup-shape frozen ground surface is increased with the increasing brine temperature and buried depth, whereas that is decreased with the increasing cup bottom thickness.

Keywords

frost-heaving characteristics, artificial ground freezing, numerical model, water-heat-force interactions, cup shape arrangement, shield tunnel

[1]School of Civil Engineering, Nanjing Forestry University
No. 159 Longpan Road, Nanjing 210037, China
*Corresponding author, email: zhanguongxing81@aliyun.com

1 Introduction

The originating and arriving of shield machine are the largest risk during shield tunnel construction, in which reinforcing end soil mass is a key influencing factor for securing the construction [1, 2]. In the weak and rich aqueous formation, the AGF is a common treatment for reinforcing the end soil mass [3, 4], since the artificial frozen wall in AGF owns not only high strength but also excellent effect of largely resisting the soil and water pressure and completely isolating water from ground contact. In view of previously published literatures, several researches on frost-heaving deformation of ground surface have been implemented using various approaches of theory, experiment and numerical simulation [5–7], in which input data involves many complex parameters in the analysis [8]. However, the arrangement of freezing pipes is sometimes varied due to various complex limitations, and the corresponding frost-heaving characteristics of ground surface also differs from others, which is also affected by complex factors such as temperature, formation properties, moisture content, load as well as boundary conditions [9]. Therefore, the frost-heaving characteristics of ground surface is difficult to be identified, and further studies are thus required for predicting the frost-heaving characteristics of ground surface in AGF.

In this paper, a case of artificial freezing end soil mass with cup shape arrangement of horizontal freezing pipes is studied, which focuses on the influences of frost-heaving characteristics of ground surface from factors of brine temperature, buried depth and cup bottom thickness, and a numerical model coupled with water-heat-force interactions is also proposed for numerical analysis.

2 Reinforcing Work Using Artificial Ground Freezing

The end soil mass with originating of shield machine is located in the intersection of two busy roads, the reinforcing work of which is implemented using AGF with cup shape arrangement of horizontal freezing pipes in the stratum silty clay, due to restriction of surrounding environment and non-affection of road transportation.

Fig. 1 shows the schematic arrangement of horizontal freezing pipes, in which 53 horizontal freezing holes are prepared. In the horizontal-cup-shape frozen area, freezing pipes in the cylinder wall are arranged along a 3750mm-radius circle with 760mm hole spacing, and those in the cup bottom are respectively arranged along 2550mm-radius and 1350mm-radius circles with uneven spacing from 1140mm to 1210mm. Moreover, the thicknesses of cylinder wall and cup bottom are respectively not less than 1200mm and 2000mm.

In the whole period of artificial freezing soil mass, the average temperature of frozen wall should be less than –10℃, in which the controlled temperature of brines in active freezing period is from –28℃ to –30℃, that in maintaining freezing period is appropriately adjusted from –25℃ to –28℃ thereafter, and the active freezing period should be not less than 40 days.

Moreover, three monitoring points of DJ8, DJ19 and DJ30 are arranged for monitoring ground surface deformation, which are 1.5m, 5m and 9m distance from originating position of shield machine as demonstrated in Fig. 2.

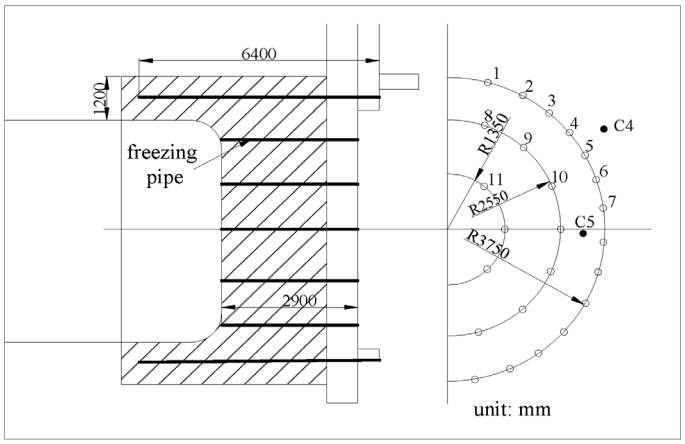

Fig. 1 Schematic arrangement of horizontal freezing pipes

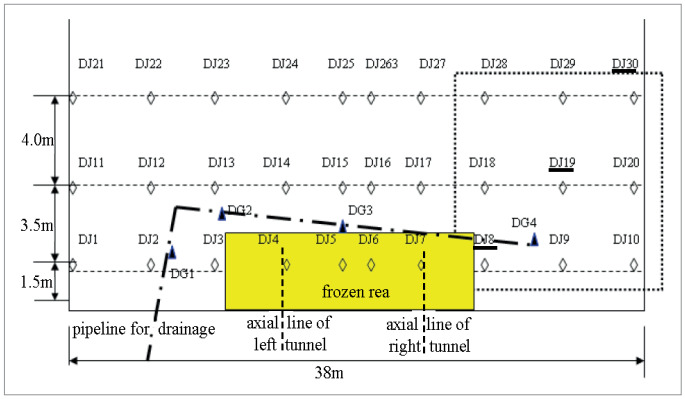

Fig. 2 Diagram of monitoring points for ground surface deformation

The physical and mechanical properties of frozen stratum are obtained from experiment and listed in Table 1, which are also compared with the undisturbed stratum. It can be clearly seen the frozen silty clay is 20 times the cohesion force of undisturbed silty clay, whereas the internal friction angle of frozen silty clay is a little decreased from that of undisturbed silty clay.

Table 1 Physical and mechanical properties of stratum

stratum	undisturbed silty clay	Frozen silty clay
frost heaving ratio (%)	--	13
bulk density (kN/m^3)	20.1	21.3
Poisson's ratio	0.27	0.25
compression modulus (MPa)	20	150
cohesion force (kPa)	50	1000
internal friction angle (°)	25	22

3 Numerical Model for Evaluating Frost-Heaving Deformation of Ground Surface

3.1 Numerical model and boundary conditions

Fig. 3 demonstrates the schematic model for the numerical analysis, in which a half calculation area is adopted due to symmetry. The numerical simulation is implemented using ADINA software [10]. In the model, the upper boundary is extended to the ground surface, the calculation range in longitudinal direction is $5R + L$, and those of lateral sides in vertical and horizontal directions are $5R + H$ and $5R$ respectively, in which R is radius of shield tunnel, H is buried depth of the tunnel, and L is length of cylinder wall in the cup-shape frozen area.

There are some assumptions in boundary conditions of the numerical model. The constant atmospheric temperature is applied to the upper boundary of ground surface, in which the average temperature of ground surface with 25℃ in summer and autumn of the city is adopted. Moreover, the brine temperature is applied to the boundary of freezing pipes and soil, according to following equations:

$$\lambda_f \left.\frac{\partial T}{\partial n}\right|_{r=R_0} = Q \tag{1}$$

$$Q = aQ_T T_y^b \tag{2}$$

Where Q is heat flux density (J/(m·s)), Q_T is heat dissipation coefficient of freezing pipes (J/m), a and b are coefficients from statistical analysis, T_y is temperature of brine (℃), T is temperature of frozen area around freezing pipes (℃), n is normal direction of boundary of freezing pipes and soil, R_0 is radius of freezing pipe (m).

Except the aforementioned boundary conditions, other boundaries of the model are adiabatic without heat transfer, dissipation and convection, which can be expressed as the following mathematical equation:

$$\lambda\left(\frac{\partial T}{\partial x}+\frac{\partial T}{\partial y}+\frac{\partial T}{\partial z}\right)=0 \tag{3}$$

Where λ and T are thermal conductivity and temperature respectively.

Besides, the three-dimensional temperature field of soil mass $T = f(x, y, z, t)$ at time $t = 0$ is confirmed by the following equations:

$$T_u\big|_{t=0} = T_0, \quad T_f\big|_{t=0} = f(x, y, z) \tag{4}$$

Where T_u and T_f are temperatures of unfrozen and frozen areas (℃), T_0 is initial temperature of soil mass (℃), and $f(x, y, z)$ is average temperature of frozen wall obtained by linear interpolation (℃)..

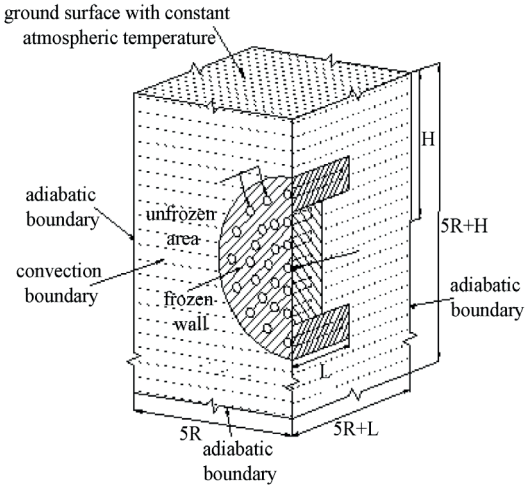

Fig. 3 Load-displacement curves

3.2 Constitutive law coupled with water-heat-force interactions

In the numerical analysis, the frost-heaving deformation is regarded as the expansion deformation induced from varied temperature field of frozen area, caused by heat conduction carried by freezing pipes, which can be expressed as the following differential equation:

$$\frac{\partial t}{\partial \tau} = \alpha \nabla^2 + \frac{\mathrm{d}\Phi}{\rho c} \tag{5}$$

$$\nabla^2 = \frac{\partial^2 t}{\partial^2 x} + \frac{\partial^2 t}{\partial^2 y} + \frac{\partial^2 t}{\partial^2 z} \tag{6}$$

Where ∇^2 is Laplace operator, α is the thermal diffusivity (m^2/s), ρ is density of ground (kg/m^3), c is specific heat (kJ/(kg·℃)), Φ is freezing cold.

In the phase-change interface between frozen and unfrozen areas, the continuous condition and energy conservation condition should be met, which can be expressed by the following equations (7) and (8):

$$T_f(s(t), t) = T_u(s(t), t) = T_m \tag{7}$$

$$\lambda_f \frac{\partial T_f}{\partial n} - \frac{\partial T_u}{\partial n} = L \frac{ds(t)}{dt} \tag{8}$$

Where T_m is phase transition temperature (℃), $s(t)$ is function of phase-change interface at time t, T_f and T_u are temperatures of frozen and unfrozen areas (℃), λ_f and λ_u are thermal conductivities of frozen and unfrozen areas (W/(m·K)), $\partial T/\partial n$ is thermal gradient (K/m) , L is latent heat (kJ/kg).

Moreover, the thermal conductivity and ground latent heat are as follows:

$$\lambda^* = \begin{cases} \lambda_f, T \prec T_m - \Delta T \\ \left(\lambda_f + \lambda_u\right)/2, T_m - \Delta T \le T \le T_m \\ \lambda_u, T \succ T_m \end{cases} \tag{9}$$

$$Q = L' \times \rho_d \times (\omega - \omega_u) \tag{10}$$

Where ΔT is temperature change of phase-change interface (℃), Q is latent heat from phase change (kJ/kg), L' is latent heat from crystallizing or melting of water (334.56 kJ/kg), ρ_d is dry density of soil mass (kg/m^3), w is total moisture content of soil, w_u is unfrozen moisture content of frozen soil.

The frost heaving behavior of frozen soil is mainly affected by moisture migration in the frozen soil, which is little influenced by in-situ pore water. Therefore, the transient coupling process of temperature field and moisture field can be simplified as quasi steady state process with small increment step of time, and the water inflow velocity thus can be expressed by the average inflow water between times t_1 and t_2, in which the inflow water q shows proportional relation to square root of time

$$dW_1 = \frac{q_2 - q_1}{t_2 - t_1} \tag{11}$$

Where dW_1 is average velocity of inflow water (m^3/s), q_1 and q_2 are inflow waters corresponded to times t_1 and t_2 (m^3).

In view of experimental investigation, inflow water are influenced by frozen time, load and frozen temperature, and inflow water shows proportional relation to square root of frozen time and exponential relation to load, which thus can be expressed by following equation:

$$q = \frac{a - bT}{a - bT_0}\left(m\sqrt{t} + n\right) \times e^{-\alpha P} \tag{12}$$

Where q is inflow water (m^3), t is frozen time (h), T and T_0 are temperature and initial temperature (℃), m and n are constants related to soil property and boundary condition, a and b are constants related to temperature, α is constant related to load. In this study, m and n take 0.0636 and -0.0827, a and b take 12.2 and 0.357, α takes 0.02, which are obtained from experimental investigation.

4 Analysis of Frost-Heaving Characteristics of Artificial Freezing End Soil Mass

In this section, the frost-heaving characteristics of above-described case of artificial freezing end soil mass are numerically analyzed, in which the horizontal freezing pipes are schematically arranged with cup shape. The numerical analysis focuses on the influences of frost-heaving characteristics of ground surface from factors of brine temperature, buried depth and cup bottom thickness in the artificial freezing end soil mass with cup shape arrangement of horizontal freezing pipes.

4.1 Calibration of the proposed numerical model

Fig. 4 shows the numerical and measured vertical displacements of ground surface at aforementioned three monitoring points of DJ8, DJ19 and DJ30, in which the numerical results demonstrates similar trend with the measured ones. The vertical displacements of DJ8, DJ19 and DJ30 with 45 frozen days are 14 mm, 5.1 mm and 2.5 mm respectively, which means the obtained vertical displacements of monitoring points are obviously decreased with the increasing distance from horizontal-cup-shape frozen area.

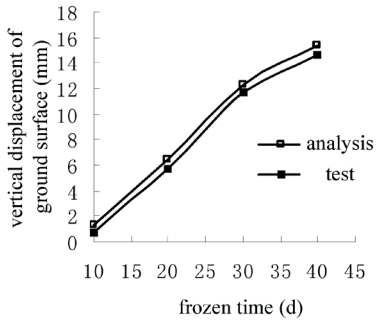

(a) DJ8

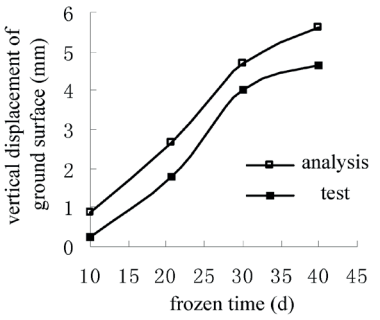

(b) DJ19

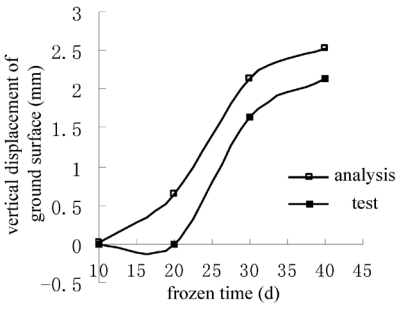

(c) DJ30

Fig. 4 numerical and measured vertical displacements of ground surface

4.2 Analytical scheme

Fig. 5 shows path scheme for studying frost-heaving characteristics of ground surface, in which paths 1 and 2 are chosen for analyzing the frost-heaving characteristics of artificial freezing end soil mass. In the scheme, paths 1 and 2 are 0.05 m and 1.0 m away from tunnel axial line and underground continuous wall, and 7 points and 6 points are respectively selected in paths 1 and 2.

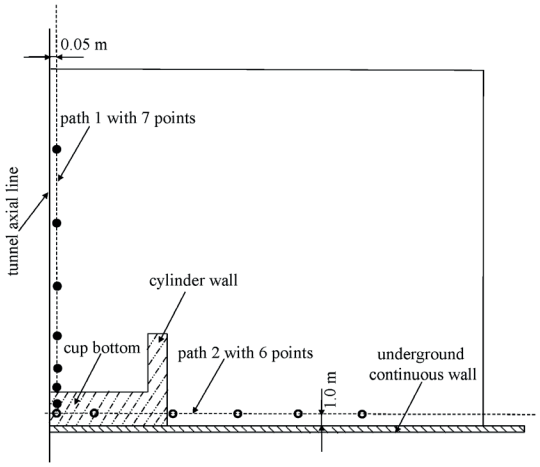

Fig. 5 Path scheme for numerical studying

4.3 Result of frost-heaving behavior of ground surface affected by brine temperature

Fig. 6 shows the vertical frost-heaving displacement of ground surface along path 2, considering the influence of brine temperature. Under condition of the same brine temperature, the vertical frost-heaving displacement of ground surface is decreased with the increasing distance from tunnel axial line, since transferred freezing cold from artificial freezing pipes is declined with increasing distance from tunnel axial line. Moreover, the maximum vertical frost-heaving displacement of ground surface is achieved with brine temperature of -16 ℃, since the moisture migration is significantly decreased and unfrozen water is accordingly reduced with lower brine temperature.

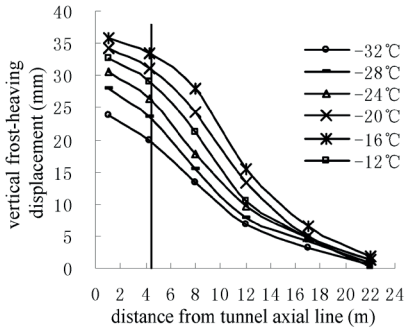

(a) Vertical frost-heaving displacement

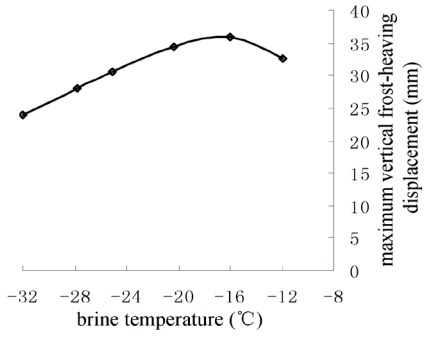

(b) Maximum vertical frost-heaving displacement

Fig. 6 Vertical frost-heaving displacement along path 2 influencing by brine temperature

Fig. 7 demonstrates the vertical frost-heaving displacement of ground surface along path 1, considering the influence of brine temperature. Under condition of the same brine temperature, the vertical frost-heaving displacement of ground surface is firstly increased with increasing distance from underground continuous wall, and then exponentially decreased after achieving the peak vertical frost-heaving displacement, which can be ignored at the distance far from underground continuous wall, since the transferred freezing cold from artificial freezing pipes is declined with increasing distance from underground continuous wall.

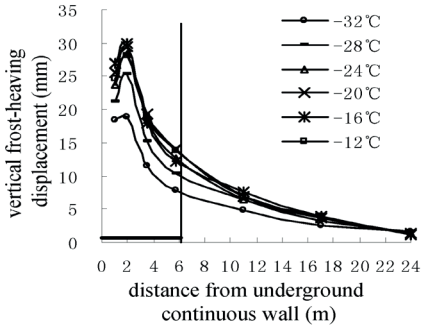

(a) Vertical frost-heaving displacement

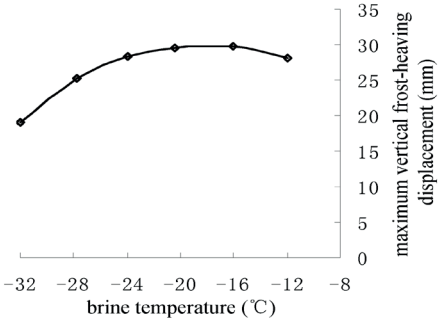

(b) Maximum vertical frost-heaving displacement

Fig. 7 Vertical frost-heaving displacement along path 1 influencing by brine temperature

4.4 Result of frost-heaving behavior of ground surface affected by buried depth

Fig. 8 shows the vertical frost-heaving displacement of ground surface along path 2, considering the influence of buried depth. Under condition of the same buried depth, the vertical frost-heaving displacement of ground surface firstly shows similar trend with Peck curve and linearly decreases thereafter. Besides, the maximum vertical frost-heaving displacements for path 2 are also exponentially decreased with increasing buried depth.

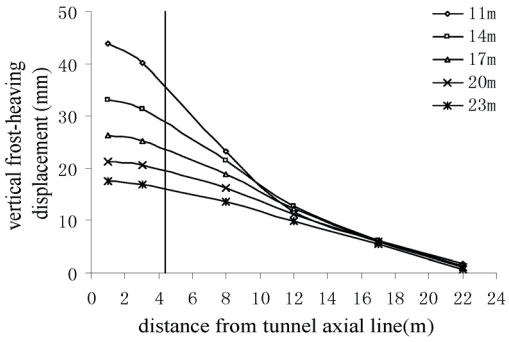

(a) Vertical frost-heaving displacement

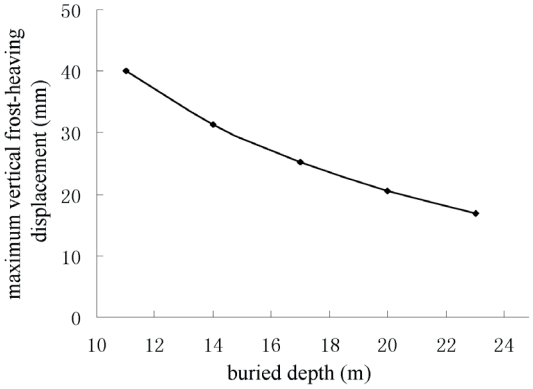

(b) Maximum vertical frost-heaving displacement

Fig. 8 Vertical frost-heaving displacement along path 2 influencing by buried depth

Fig. 9 shows the vertical frost-heaving displacement of ground surface along path 2, considering the influence of buried depth. It also can be clearly seen the vertical frost-heaving displacement of ground surface under condition of the same buried depth is firstly increased with increasing distance from underground continuous wall, and then exponentially decreased after achieving the peak vertical frost-heaving displacement, which can be ignored at the distance far from underground continuous wall. Moreover, the vertical frost-heaving displacement of ground surface is reduced with increasing buried depth, whereas it is little affected by buried depth at the distance far from underground continuous wall. Besides, the maximum vertical frost-heaving displacements for path 1 are also exponentially decreased with increasing buried depth.

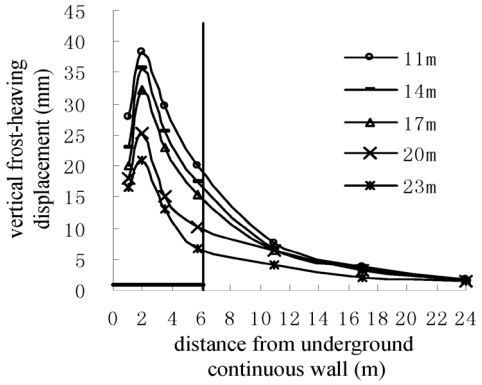

(a) Vertical frost-heaving displacement

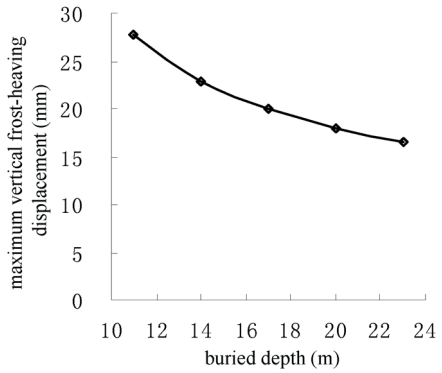

(b) Maximum vertical frost-heaving displacement

Fig. 9 Vertical frost-heaving displacement along path 1 influencing by buried depth

4.5 Result of frost-heaving behavior of ground surface affected by cup bottom thickness

Fig. 10 shows the vertical frost-heaving displacement of ground surface along path 2, considering the influence of cup bottom thickness. Under condition of the same cup bottom thickness, the vertical frost-heaving displacement of ground surface is decreased with the increasing distance from tunnel axial line, which also shows similar trend with Peck curve. Besides, the maximum vertical frost-heaving displacement for path 2 is reduced-incrementally increased with increasing cup bottom thickness.

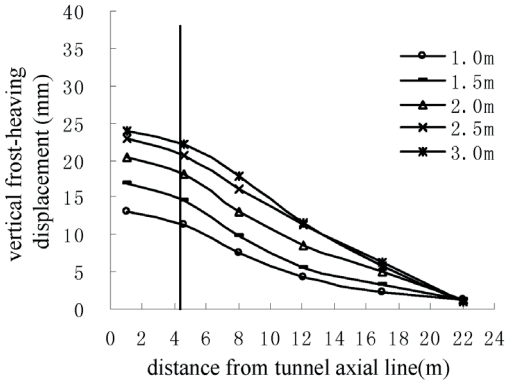

(a) Vertical frost-heaving displacement

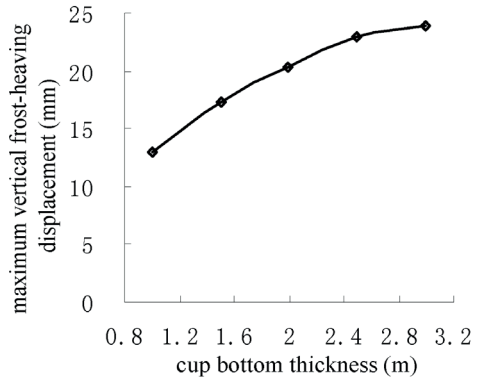

(b) Maximum vertical frost-heaving displacement

Fig. 10 Vertical frost-heaving displacement along path 2 affected by cup bottom thickness

Fig. 11 demonstrates the vertical frost-heaving displacement of ground surface along path 1, considering the influence of cup bottom thickness. Under condition of the same cup bottom thickness, the vertical frost-heaving displacement of ground surface is firstly increased with increasing distance from underground continuous wall, and then exponentially decreased after achieving the peak vertical frost-heaving displacement, which also can be ignored at the distance far from underground continuous wall. Besides, the maximum vertical frost-heaving displacement for path 1 is also reduced-incrementally increased with increasing cup bottom thickness.

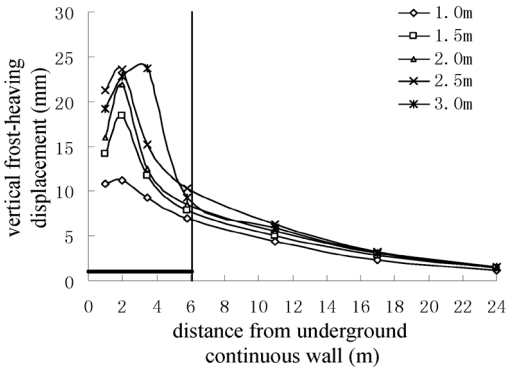

(a) Vertical frost-heaving displacement

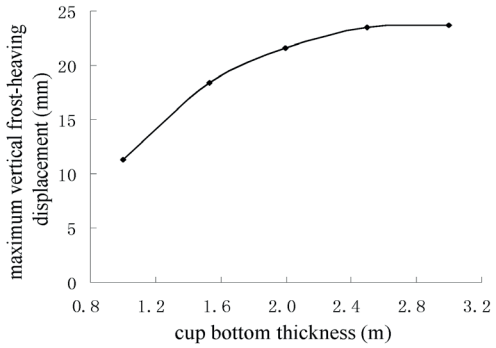

(b) Maximum vertical frost-heaving displacement

Fig. 11 Vertical frost-heaving displacement along path 1 affected by cup bottom thickness

5 Conclusions

In this paper, a case of artificial freezing end soil mass for safe arriving of shield machine is studied, in which the horizontal freezing pipes are schematically arranged with cup shape, and a numerical model is proposed for predicting the frost-heaving characteristics of ground surface in artificial freezing method.

(1) The proposed numerical model coupled with water-heat-force interactions can appropriately evaluate the frost-heaving characteristics of ground surface in artificial freezing method, the effectiveness of which is confirmed by the conformed results from experimental investigation and numerical analysis.

(2) In the artificial freezing method with cup shape arrangement of horizontal freezing pipes, the factors of brine temperature, buried depth and cup bottom thickness have significantly influences of frost-heaving characteristics of ground surface.

(3) In the path parallel to tunnel axial line, the vertical frost-heaving displacements of ground surface affected by brine temperature, buried depth and cup bottom thickness demonstrate similar trends, all of which are firstly increased with increasing distance from underground continuous wall, and then decreased after achieving the peak vertical frost-heaving displacement.

(4) In the path parallel to underground continuous wall, the vertical frost-heaving displacements of ground surface affected by brine temperature, buried depth and cup bottom thickness also demonstrate similar trends, all of which are decreased with the increasing distance from tunnel axial line and show similar trends with Peck curve.

Acknowledgement

The project presented in this article is supported by National Natural Science Foundation of China (51478226, 51578292), and Natural Science Foundation of Jiangsu Province (BK20140629).

References

[1] Fang, Y., Yang, Z. H., Cui, G., He, C. "Prediction of surface settlement process based on model shield tunnel driving test." *Arabian Journal of Geosciences*. 8 (10), pp. 7787–7796. 2015. DOI: 10.1007/s12517-015-1800-0

[2] Hu, X. D., Guo, W., Zhang, L. Y., Wang, J. T. "Application of liquid nitrogen freezing to recovery of a collapsed shield tunnel." *Journal of Performance of Constructed Facilities*. 28 (4), pp. 757-766. 2014. DOI: 10.1061/(ASCE)CF.1943-5509.0000477

[3] Alexandrov, V. N., Filonov, V. A., Maslak, V. A. "Zone nitrogen freezing of technological boreholes in the Saint Petersburg metro." In: Proceedings of the AITES-ITA World Tunnel Congress, Milan, Italy. Vol. 3, pp. 13–20. 2001.

[4] Heidkamp, H., Katz, C., Hofsstetter, C. "Enlargement of the Marienplatz metro station - a complex tunnel project beneath Munich city hall." *Structural Engineer*. 84 (3), pp. 41–44. 2006. URL

[5] Gutkin, Y. M. "Horizontal frost-induced heaving pressure of clayey soils on enclosing structures of finite stiffness." *Soil Mechanics & Foundation Engineering*. 51 (1), pp. 44–51. 2014. DOI: 10.1007/s11204-014-9253-0

[6] Bronfenbrener, L., Bronfenbrener, R. "Frost heave and phase front instability in freezing soils." *Cold Regions Science and Technology*. 64 (1), pp. 19–38. 2010. DOI: 10.1016/j.coldregions.2010.07.001

[7] Peterson, R. A. "Stability analysis and numerical simulation of differential frost heave." *Mathematical Geosciences*. 40 (3), pp. 277–298. 2008. DOI: 10.1007/s11004-008-9150-z

[8] Konrad, J. M. "Estimation of the segregation potential of fine-grained soils using the frost heave response of two reference soils." *Canadian Geotechnical Journal*. 42 (1), pp. 38–50. 2005. DOI: 10.1139/t04-080

[9] Yang, P., Ke, J. M., Wang, J. G., Chow, Y. K., Zhu, F. B. " Numerical simulation of frost heave with coupled water freezing, temperature and stress fields in tunnel excavation." *Computers & Geotechnics*. 33 (6–7), pp. 330–340. 2006. DOI: 10.1016/j.compgeo.2006.07.006

[10] ADINA. ADINA R&D, Inc..